Fine-scale damage estimates of particulate matter air pollution reveal opportunities for location-specific mitigation of emissions

Andrew L. Goodkind[a,1], Christopher W. Tessum[b], Jay S. Coggins[c], Jason D. Hill[d], and Julian D. Marshall[b]

[a]Department of Economics, University of New Mexico, Albuquerque, NM 87131; [b]Department of Civil and Environmental Engineering, University of Washington, Seattle, WA 98195; [c]Department of Applied Economics, University of Minnesota, St. Paul, MN 55108; and [d]Department of Bioproducts and Biosystems Engineering, University of Minnesota, St. Paul, MN 55108

Fine particulate matter ($PM_{2.5}$) air pollution has been recognized as a major source of mortality in the United States for at least 25 years, yet much remains unknown about which sources are the most harmful, let alone how best to target policies to mitigate them. Such efforts can be improved by employing high-resolution geographically explicit methods for quantifying human health impacts of emissions of $PM_{2.5}$ and its precursors. Here, we provide a detailed examination of the health and economic impacts of $PM_{2.5}$ pollution in the United States by linking emission sources with resulting pollution concentrations. We estimate that anthropogenic $PM_{2.5}$ was responsible for 107,000 premature deaths in 2011, at a cost to society of $886 billion. Of these deaths, 57% were associated with pollution caused by energy consumption [e.g., transportation (28%) and electricity generation (14%)]; another 15% with pollution caused by agricultural activities. A small fraction of emissions, concentrated in or near densely populated areas, plays an outsized role in damaging human health with the most damaging 10% of total emissions accounting for 40% of total damages. We find that 33% of damages occur within 8 km of emission sources, but 25% occur more than 256 km away, emphasizing the importance of tracking both local and long-range impacts. Our paper highlights the importance of a fine-scale approach as marginal damages can vary by over an order of magnitude within a single county. Information presented here can assist mitigation efforts by identifying those sources with the greatest health effects.

air pollution | environmental economics | marginal damages | particulate matter

Exposure to air pollution is linked to many serious health effects, including respiratory infections, lung cancer, stroke, and cardiopulmonary disease (1–3), all of which come at great economic cost (4, 5). The overwhelming majority of estimated monetized damages from air pollution is attributable to premature mortality (5); the main contributor is $PM_{2.5}$. Ambient concentrations of $PM_{2.5}$ in the United States have fallen in recent decades, but devising and prioritizing strategies for efficiently reducing emissions, exposures, and health impacts will yield large additional benefits. Efficient approaches commonly target those sources with the lowest mitigation costs [i.e., economic costs per ton (t) emissions avoided] and the greatest marginal damages [i.e., economic damages t^{-1} emitted]. Here, we focus on the latter. The health impact of a given quantity of emissions depends on where it was emitted and where it travels as well as on the physical and chemical transformations that generate and remove $PM_{2.5}$ as it moves through the atmosphere. Marginal damage also depends in part on "intake fraction" [i.e., the fraction of emissions that are inhaled (6)], which varies by orders of magnitude among sources, depending on the size and proximity of populations to sources, and on the persistence of the pollution.

Here, we use the Intervention Model for Air Pollution (InMAP) to calculate location-specific estimates of the marginal damages of emissions from all emission locations in the contiguous United States (7). These estimates form a series of matrices that describe linear relationships among multiple emission and impact locations; we call this InMAP Source-Receptor Matrix (ISRM). We consider emissions of primary $PM_{2.5}$ and of four chemical species—ammonia (NH_3), nitrogen oxides (NO_x), sulfur dioxide (SO_2), and volatile organic compounds (VOCs)—that react to form secondary $PM_{2.5}$ in the atmosphere.

This novel approach integrates a fine spatial scale with information on the long-range transport of emissions, producing results with finer resolution in densely populated urban areas (as small as 1 km × 1 km) and coarser resolution in rural areas (as large as 48 km × 48 km) for greater computational efficiency. This approach allows us to identify large spatial gradients in marginal damages that result from emission location and to model the substantial impacts of emissions experienced far downwind of sources.

We present our results in terms of the incidence of premature mortality attributable to exposure to $PM_{2.5}$ and the monetary valuation (or damages) of these deaths. Calculating damages from individual sources of emissions requires three steps: (i) tracing the air quality impacts of emissions to downwind receptors, (ii) converting changes in pollution exposure to changes in mortality, and (iii) applying a monetary valuation for changes in

Significance

Health burdens of $PM_{2.5}$ and its precursors vary widely depending on where emissions are released. Thus, advanced methods for assessing impacts on a fine scale are useful when developing strategies to efficiently mitigate the effects of air pollution. We describe a new tool for rapidly assessing the impacts of pollution emissions on a fine scale. We apply the tool to the US emissions inventory to better understand the contribution of each economic sector on reduced air quality. We show that, even for a national assessment, local (e.g., subcounty) information is important to capture the variability in health impacts that exist on fine scales. Our paper can help policymakers and regulators prioritize mitigation of emissions from the most harmful source locations.

ENVIRONMENTAL SCIENCES

SUSTAINABILITY SCIENCE

the risk of mortality. Our key contribution is in step *i*, which encompasses providing location-specific fine-scale estimates of the mortality effects of $PM_{2.5}$ from marginal changes in emissions, tracing the health impacts back to where the emissions occurred, and applying the results to a national emission inventory, so as to quantify the impacts of specific emission sources and emission locations throughout the United States. Methods we employ for steps *ii* and *iii* are straightforward state-of-knowledge approaches: a linear concentration-response (C-R) function that estimates changes in mortality from changes in exposure to $PM_{2.5}$ (8) and the value of a statistical life (VSL) (9) to translate increased mortality into monetary damages (see *Methods* and *SI Appendix*, section S1 for details). The use of monetized damages provides a broader context for understanding our estimates of exposure and of the impact of emissions and helps us compare our results with existing estimates in the literature (10, 11).

Results

Our results are in five sections. First, we estimate the monetary marginal damages ($ t^{-1}) at every emission source location in the United States. Those findings, which are the core of the ISRM, reveal the locations where a one-unit change in emissions will have the greatest impact on health. Second, we combine those results ($ t^{-1}) with the National Emissions Inventory (i.e., t emitted) to understand total damages by emission location. Third, we explore total damages per sector of the economy. Fourth, we estimate where damages occur in terms of distance from each emission location. Fifth, we provide model validation and uncertainty analysis.

Marginal Damages. Here, we estimate the marginal damages of emissions at every source location in the United States. Damages attributable to emissions at a specific location vary by pollutant and release height; we show here (Fig. 1) results for the most common release height for each pollutant (ground level for primary $PM_{2.5}$, NH_3, NO_x, and VOC; high stacks for SO_2). (Results for other release heights are in the *SI Appendix*, Table S1.) For each pollutant, marginal damages vary widely among source locations with marginal damages generally being higher for emissions released near population centers. Pearson correlation coefficients between population density at the emission location and marginal damages are highest for $PM_{2.5}$ and NH_3 emissions (0.76 and 0.74, respectively) and lowest for SO_2 emissions (0.13). The relatively low correlation for SO_2 occurs because this type of emission more frequently comes from high stacks and more time is required in the atmosphere for it to form secondary $PM_{2.5}$, leading to a greater share of its impacts occurring far downwind of the source. Primary $PM_{2.5}$, on the other hand, is often released at ground level and is already in fine particle form; consequently, a greater share of its impacts occurs near the source.

Average marginal damages t^{-1} emitted are \$94,000 for primary $PM_{2.5}$, \$40,000 for NH_3, \$13,000 for NO_x, \$24,000 for SO_2, and \$7,500 for VOC. The distributions of marginal damages exhibit positive skew, suggesting that a small quantity of emissions at the right tail of the distribution has very large marginal damages (*SI Appendix*, Table S1).

Combining Marginal Damages with the National Emission Inventory. The previous section considers impacts per t emitted (ISRM); here, we combine the ISRM with estimates of actual emissions (t), taken from the US Environmental Protecton Agency (EPA) 2011 National Emissions Inventory (NEI) (12) to reveal total damages. We then calculate the distribution of marginal damages, weighted by the quantity of anthropogenic emissions from each grid cell. We find that the marginal damages of emissions vary widely by source location and that emissions from the highest marginal damage sources, although low in total mass, account for a large share of total emission damages. That finding emphasizes the importance of considering sources in terms of their impact, not
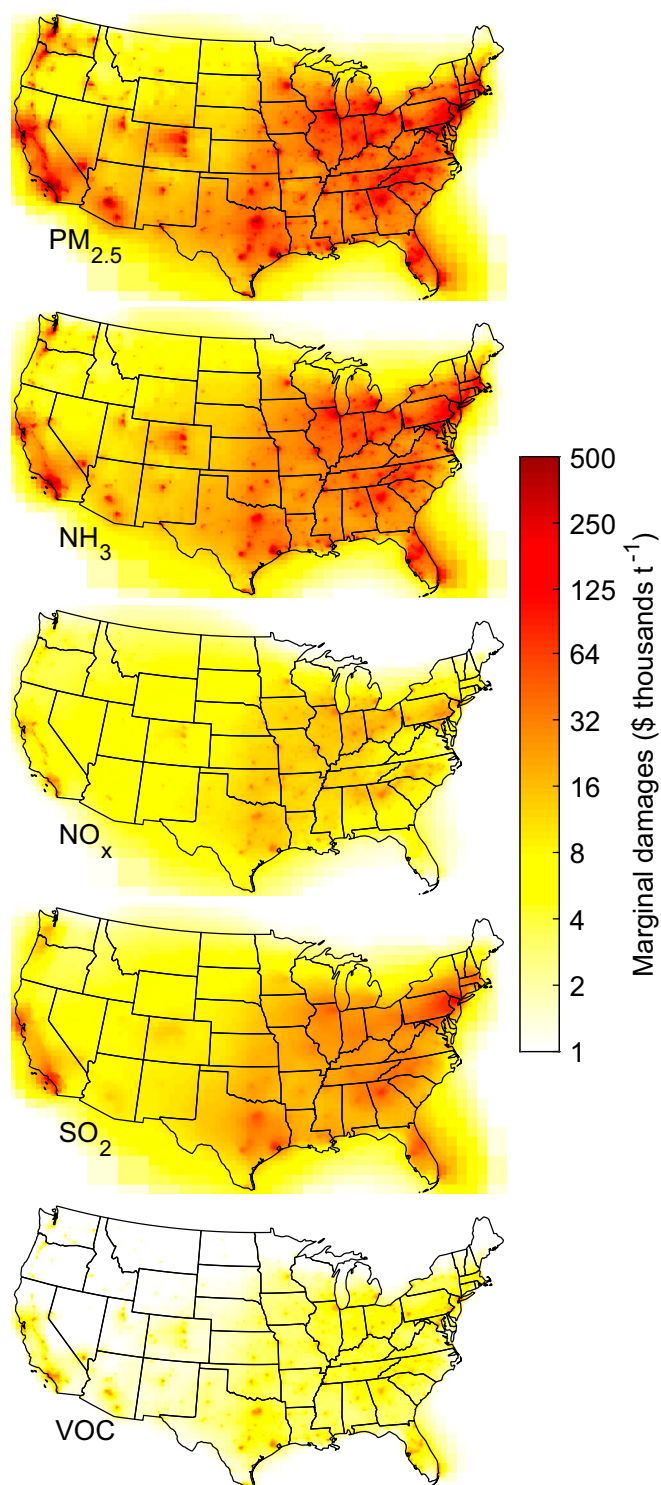
Fig. 1. Marginal damages of emissions ($ t^{-1}; logarithmic scale) by emitted pollutant and emission location. Damages are generally higher for emissions upwind of population centers, but the relationship with population density varies by pollutant. The value displayed in a location represents the combined mortality impacts (in terms of dollar damages) to all downwind receptors from 1 t emitted at that location.

just emissions. Impacts, measured as mortality and as monetary damages per t of emissions, can vary by an order of magnitude within a single county. The most harmful emissions per t are responsible for a substantial share of the total damages. For example,

Los Angeles, CA   Seattle, WA

Primary PM$_{2.5}$ marginal damages ($ thousands t^{-1})

4   8   16   32   64   125   250   500   1,000   2,000

Fig. 2. Within-urban and within-county variability in marginal damages ($ t^{-1}; logarithmic scale) of primary PM$_{2.5}$ emissions in the Los Angeles, CA and Seattle, WA regions. The black lines represent county boundaries.

the top 1% and 10% most harmful primary PM$_{2.5}$ emissions are responsible for 17% and 54% of the total primary PM$_{2.5}$ damages, respectively. The damage per t of primary PM$_{2.5}$ for the 1% most harmful emissions is over $900,000—on average, every five t of these emissions are estimated to cause one additional case of premature mortality—a 400-fold greater premature mortality rate per t than that associated with the least harmful 1% of primary PM$_{2.5}$ emissions ($4,200 t^{-1}; 2,000 t per premature mortality). The top 10% highest marginal damage emissions of NH$_3$, NO$_x$, SO$_2$, and VOC account for 42%, 27%, 21%,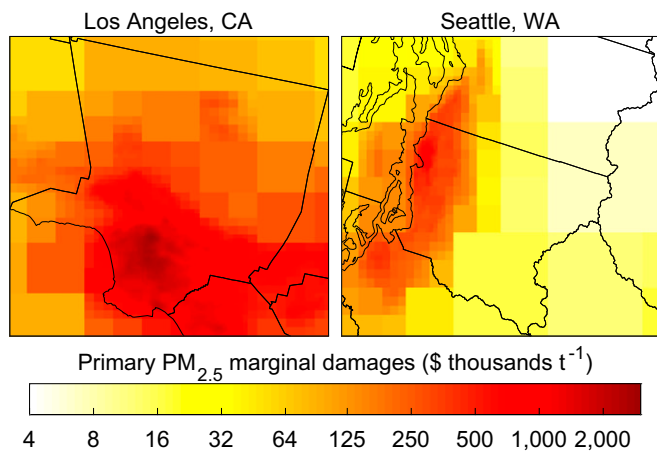 and 37% of the total damages for each pollutant, respectively. For PM$_{2.5}$ and VOC, the most-damaging 10% of emissions mass is ∼15× more harmful (for NH$_3$, NO$_x$, and SO$_2$, ∼5× more harmful) than the 10% least-damaging emissions mass.

The highest marginal damage emissions are concentrated almost exclusively in high-population-density areas. InMAP's variable-grid-cell design can resolve intraurban-scale spatial gradients in damages; a gradient map at this spatial scale has not previously been produced for national-scale location-specific estimates (10, 11). Here, we explore within-county variation in marginal damages in terms of the ratio of the marginal damages in the most- to least-damaging ground-level emission locations within each county. In the 10% most densely populated counties—comprising 58% of the total US population—the average marginal damage ratio within a county is 8.1 for primary PM$_{2.5}$, 6.7 for NH$_3$, 3.4 for NO$_x$, 1.8 for SO$_2$, and 5.8 for VOC. That is, in these densely populated counties, primary PM$_{2.5}$ is on average ∼8× more harmful per unit in one location than in another location within the same county. As an illustration, Fig. 2 shows the heterogeneity in marginal damages for emissions in two large metropolitan areas: Los Angeles and Seattle. For Los Angeles County, CA, InMAP uses >1,000 grid cells; estimated marginal damages range from $52,000 to $2,900,000 t^{-1} for primary PM$_{2.5}$ (i.e., a 56-fold difference). For King County, WA (which contains Seattle, WA), InMAP uses 374 grid cells, and the marginal damages for primary PM$_{2.5}$ span a 127-fold range: $7,000 to $890,000 t^{-1}.

Total estimated annual damages from anthropogenic PM$_{2.5}$ are $886 billion, corresponding to 107,000 cases of premature mortality. Primary PM$_{2.5}$ constitutes the largest share of damages (38%); the four other pollutants are each associated with 12–19% of total damages.

Damages by Economic Sector. Connecting the ISRM with an emissions inventory enables us to next explore the damages by economic sector and the variability of damages within a sector.

Total damages and incidence of premature mortality by pollutant, economic sector, and emission height (left and right axes, respectively, of Fig. 3) reveal the multifaceted nature of this environmental risk factor: Many sources and pollutants contribute meaningfully to total PM$_{2.5}$. Ground-level emissions dominate total impacts, of which primary PM$_{2.5}$ is the largest contributor. The single largest contribution to total anthropogenic damages (in Fig. 3) is ground-level release of NH$_3$ from agriculture (i.e., application and storage of manure; fertilizer use), contributing 12% of total impacts. Among impacts from elevated emissions, SO$_2$ from coal-fired power plants is the largest contributor, responsible for 58% of total damages from elevated emissions (11% of total damages). Combining major sources associated with energy consumption [e.g., transportation (28%), electricity generation (14%)] constitutes 57% of total impacts. Although total damages from emissions of NH$_3$ and SO$_2$ are each dominated by a single sector (NH$_3$: agriculture; SO$_2$: coal-fired power plants), total damages from emissions of primary PM$_{2.5}$, NO$_x$, and VOC are not. As no one economic sector dominates total damages, sizable reductions to PM$_{2.5}$ air pollution requires focusing on many sources of pollution. (See *SI Appendix*, Tables S2 and S3 for total and marginal damages by disaggregated sectors.)

Next, we build on the sector-specific estimates by exploring within-sector distributions of marginal damages. Analogous to the findings above, here we find that, for a given sector and pollutant, marginal damages by sources often exhibit a wide range of values. For example, for gasoline-vehicle VOC, the 10% most-damaging emission locations have marginal damages greater than $22,000 t^{-1}, whereas the 10% least-damaging locations have marginal damages less than $2,200 t^{-1}, a gap of more than 10×. The 10th to 90th percentile range for marginal damages is $12,000–$320,000 t^{-1} for locations of primary PM$_{2.5}$ from residential wood burning (difference: >26×), $10,000–$58,000 t^{-1} for NH$_3$ emission locations from agriculture (>5×), $11,000–$33,000 t^{-1} for SO$_2$ emission locations from coal-fired electric power plants (3×), and $5,200–$29,000 t^{-1} for NO$_x$ emission locations from on-road diesel vehicles (>5×). For a specific sector or pollutant, there are potentially large health advantages and efficiency gains from targeting the highest-impact locations. This aspect is especially relevant for difficult-to-control sectors, such as agriculture, road dust, and residential
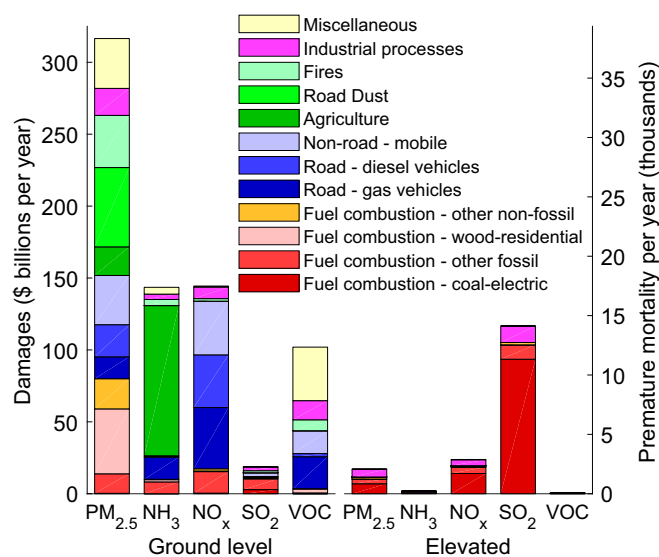

Fig. 3. Total damages and attributable premature mortality associated with anthropogenic emissions in 2011 ($ billions) by sector, pollutant, and emission height.

Fig. 4. Cumulative damages by pollutant and distance of impacted populations from sources of anthropogenic emissions. The black dashed line at 32 km from the source represents the distance within which 50% of total damages occur.

wood burning: for those sectors, if nationwide emission controls are unlikely, an alternative approach is to target emission reductions in a small number of high-impact locations. In practical terms, this could mean focusing greater attention on local policy in high-impact locations rather than national policy.

Impacts by Distance from Source Location. Results thus far have considered total damages by emission location, source, or species. In this section, we explicitly consider where damages occur. As described next, our results emphasize that local and long-distance components are both important for estimating total health impacts from $PM_{2.5}$.

We estimate—averaging across all locations, sources, and stack heights, and including primary and secondary $PM_{2.5}$—that half of total $PM_{2.5}$ damages are incurred by people living within 32 km of a source (Fig. 4). (One-third of damages occur at locations within 8 km of the source; another one-quarter occur more than 256 km downwind of the source.) That finding emphasizes the benefits of the modeling approach employed here (InMAP and ISRM), which uses variably sized grid cells (as small as 1 km × 1 km). In contrast, a typical spatial resolution for conventional air pollution models [chemical transport models (CTMs) or reduced-complexity models] applied nationally and for annual averages is 36 km × 36 km grid cells or county level (the average land area per county in the contiguous United States is ~2,500 km², analogous to 50 km × 50 km grid cells)—too large to capture spatial gradients amounting to more than half of total damages. For environmental justice (EJ) analyses (e.g., consideration of which demographic groups inhale more or less pollution) an ability to capture near-source gradients may be especially important. In that case, a second implication of findings here is that conventional models may be too coarse to adequately investigate many EJ questions (13).

Spatial variability differs by pollutant: For primary $PM_{2.5}$, more than half of damages occur less than 16 km from the source; for SO_2, more than half are experienced by people living farther than 200 km from the source. This result suggests that finer-resolution models are more important for primary $PM_{2.5}$ and likely are less important for SO_2. Another implication is that for a community aiming to reduce its ambient $PM_{2.5}$, local (e.g., county-level) action may be more successful for primary $PM_{2.5}$ than for SO_2.

Model Validation and Uncertainty Analysis. To evaluate the reliability of our model to predict concentrations of ambient $PM_{2.5}$, we compare observed year-2011 annual-average concentrations of $PM_{2.5}$ at EPA monitoring locations (14) with predicted concentrations from the ISRM, based on emissions from the 2011 NEI (Fig. 5). Average MFB is −6%; MFE is 36%. [These values reflect the combined impact of errors in the model (ISRM), emission inventory, and meteorological inputs.] Those bias/error values, which reflect annual-average observations at the 840 monitor locations throughout the United States, are well within published air quality model performance criteria: MFB ≤ ±60%, MFE ≤ 75% (15). That result supports the use of the ISRM to predict concentrations of ambient $PM_{2.5}$. (InMAP performance is better for primary $PM_{2.5}$ and for SO_2 than for NH_3 and NO_x; details are in *SI Appendix*, section S3.2.)

We next consider, in turn, uncertainty in the three main inputs to our calculations: the ISRM, the C-R function, and the VSL. First, we characterize error in the ISRM $PM_{2.5}$ concentration predictions and resulting mortality estimates as above: based on model-measurement comparisons (Fig. 5). Specifically, for the error in each ISRM spatial prediction of $PM_{2.5}$ concentration, we employ the model-measurement error at the nearest EPA monitor (see *SI Appendix*, section S1.5 for details and 95% confidence interval estimate of mortality using similar methods). The total estimated mortality from this sensitivity analysis is 99,000, or 8% less than our base-case estimate (107,000). Errors

Fig. 5. Comparison of ISRM-predicted total $PM_{2.5}$ concentrations and observed concentrations at 840 monitor locations for year 2011. Evaluation metrics: MB, mean bias; ME, mean error; MFB, mean fractional bias; MFE, mean fractional error; best-fit slope (S), and R^2.

estimated in this method differ by sector; for example, mortality in the sensitivity analysis (relative to in the base case) is 11% lower for emissions from industrial processes but only 3% lower for coal-fired electric generation.

Second, we explore uncertainty in the C-R function, first by using a deterministic method (employing an alternative C-R function) and second by using a Monte Carlo simulation (adopting the reported 95% confidence intervals reported for regression coefficients from the underlying epidemiological study). For the first method, we replace the base-case C-R [from Krewski et al. (8)] with the C-R from Nasari et al. (16). The result is that total estimated mortality increases 21% to 129,000. This shows that our base-case estimates are of comparable magnitude but lower than the estimates using another authoritative C-R function. For the second method (Monte Carlo), the resulting 95% confidence interval [and interquartile range (IQR)] for total mortality is 44,000–171,000 (85,000–129,000).

Third, we explore uncertainty in the VSL. The VSL employed here is the mean of estimates from several studies (9). We employ a Monte Carlo analysis by using the distribution of these studies' estimates. The resulting 95% confidence interval (IQR) for total damages is $90 billion to $2.3 trillion ($460 billion to $1.2 trillion).

To summarize, 95% confidence intervals associated with the three main inputs for total damages (base-case estimate: $886 billion), in units of $billions, are 90–2,300 for the VSL, 360–1,400 for the C-R function, and 830–930 for the ISRM. (See *SI Appendix*, section S1.5 for details.) Those findings suggest that uncertainty is greatest for the VSL, smaller for the C-R function, and smallest for the ISRM.

Discussion

Here, we estimate the mortality impacts of $PM_{2.5}$ air pollution in the United States. Our approach advances the science by (*i*) developing a fine-scale source-receptor matrix (the ISRM), which simulates impacts near to the source and far from the source, (*ii*) using the ISRM to explore impacts by emission location, chemical species, and source category, and (*iii*) studying this topic nationally, with unprecedented spatial resolution. This approach was possible because of the computational efficiency of InMAP; analyses here would not be feasible with conventional CTMs (see *Methods* section).

The existing literature on intake fraction documents that damages t^{-1} can vary widely, depending on release location (17–19). Some of our results have similar utility as intake-fraction values but usefully extend beyond that literature by, for example, calculating health impacts and monetized damages, accounting for all $PM_{2.5}$ (primary and secondary) from all sectors of the economy, employing a much finer spatial resolution for a national analysis, developing the source-receptor model, and integrating the source-receptor model with the NEI.

Our estimates of total damages from anthropogenic $PM_{2.5}$ ($886 billion associated with 107,000 deaths in 2011) are similar to values reported elsewhere. For example, Fann et al. (20) estimated 130,000 deaths from $PM_{2.5}$ in 2005. The Institute for Health Metrics and Evaluation (21) estimated 90,000 US deaths from $PM_{2.5}$ in 2015. In addition, Heo et al. (11) conclude that total damages in the United States are $1.0 trillion per year, similar to our estimate. Comparisons to specific locations, sources, or chemical species may reveal larger or smaller differences. For example, we estimate ~3× higher marginal damages of SO_2 from coal-fired electricity-generating units than a report by the National Research Council (22) but find a similar geographic distribution. Our estimate of the share of total $PM_{2.5}$-related mortality from mobile sources (34%) is higher than the share from Fann et al. (23) (22%), but we estimate a similar share from electricity-generating sources [17% of total (ISRM) vs. 22% (Fann et al. (23)].

Our results emphasize the benefits of finer-scale spatial resolution, relative to the typical spatial resolution of conventional models. To further explore this issue, we recalculate our core results but using coarser fixed-size grid cells of 48 km × 48 km, rather than the smaller variably sized grid cells of our main approach (see *SI Appendix*, section S1.6 for details). Resulting estimates for total damages from $PM_{2.5}$ are ~20% lower with the coarser grid than with our main approach; analogous differences are larger for mobile sources (27% lower) and residential wood burning (34% lower) with nearly zero difference for emissions from coal-fired electricity generation. The difference with the coarser grid compared with our main approach is nearly zero for low-damage locations and for elevated sources but is relatively large for high-damage locations. For example, the highest estimated marginal damages t^{-1} for primary $PM_{2.5}$ are $523,000 (coarser grid) vs. $919,000 (main approach). Thus, the sensitivity analysis supports the use of smaller grid cells for modeling spatial variability in damages and especially for discovering high-impact locations.

The approach we present here has several limitations in addition to the uncertainties highlighted in the *Results* section. We do not account for differing effects of air pollution by season, and our model currently does not track all harmful air pollutants, such as ozone. Seasonal differentiation may be important where emissions and rates of $PM_{2.5}$ formation both vary by season [e.g., seasonal fertilizer application (agricultural emissions) in an area where ammonium or nitrates are rate-limiting species during different times of the year]. InMAP partially accounts for seasonality in how it tracks annual-average impacts, but if a location has emissions that exhibit seasonal patterns, use of an annual-average impact for that location could induce bias in the estimated impacts. This aspect is worthy of investigation and quantification using a different model than the one employed here. Exposure to ozone is also associated with increased risk of premature mortality, but those risks are generally small compared with the estimated risk from $PM_{2.5}$. For example, Fann et al. (20) estimate that attributable mortalities are ~30× greater for $PM_{2.5}$ than for ozone.

Many minor local emission sources can contribute to ambient pollution, including fireplaces, cooking, and lawn care. Our approach includes those sources, which are in the NEI, but our model does not capture near-source exposures for which the relevant exposure travel distance is much less than the length scale of our model (1 km to 48 km). Such exposures include, for example, a cook directly inhaling grilling exhaust, a pedestrian directly inhaling emissions from a nearby vehicle's exhaust plume, or lawnmower-engine exhaust being directly inhaled by the person mowing a lawn. These ultra-near-source exposures are high concentration but generally short duration. Our approach does not include direct indoor inhalation of indoor sources; in some circumstances (e.g., "second-hand" cigarette smoke), indoor exposures can dominate total exposures.

We use the VSL from the US EPA to convert changes in mortality risk to monetary damages. This approach is a common if controversial method. Other literature review estimates of the VSL are consistent with the EPA VSL employed here (24, 25). Alternative (i.e., non-VSL) valuation methods are available, for example, considering years of life lost ("value of a statistical life year") or accounting for morbidity and mortality using "disability" adjustment factors ("value of a disability-adjusted life year") (26). These are important considerations that deserve attention in future analyses.

Uncertainty is relatively large in the C-R function and in the VSL: the range of the 95% confidence intervals is a factor of 4 and a factor of 25, respectively. Such uncertainties are inherent in estimates for any one location, emission source, or pollutant; however, they do not impact the relative damages for one source compared with another source. There is potentially spatial and demographic variabilities in the C-R function and the VSL as well. For example, perhaps people in a certain neighborhood are highly susceptible to health impacts from air pollution. In that

case, emission locations that lead to pollution in that neighborhood would have greater-than-average impacts. The same may be true for certain group's valuation of increased risks of mortality. To the extent that this variability can be estimated, there is also an ethical consideration regarding how that variability should be included in the types of analyses we produce here. Similarly, as fine-scale estimates of pollution exposure become available, policies that use this information to target reductions in certain locations and not others raise important questions of fairness in environmental quality.

$PM_{2.5}$ is the largest environmental risk factor in the United States, causing >100,000 premature deaths per year—more than traffic accidents and homicides combined (27). Reducing $PM_{2.5}$ concentrations is aided by prioritizing among emission sources: which sources to reduce and by how much. The fine-scale damage estimates given here reveal new opportunities for location-specific mitigation of emissions. However, any policy implementation would need to consider trade-offs between the benefits of targeted emission reductions and the additional regulatory burden caused by location-specific policy. The ISRM is novel in connecting ambient concentrations and damages with the emission locations, sources, and species causing those concentrations and damages nationally and at a spatial resolution not previously possible. The new spatial resolution reveals, at a national level, large spatial gradients in damages, including within county and within urban. These new results are useful for (*i*) more-efficient environment policy (i.e., using emission-reduction policies, permitting decisions, and enforcement actions to reduce highest-impact sources, locations, and species), (*ii*) investigating EJ (i.e., understanding which groups are more/less exposed and proposing policies to address potential undue burdens), and (*iii*) correctly estimating the magnitude of damages because results here account for near-source and long-range exposures. We have made the ISRM freely available online (28) with the hope that researchers and practitioners will find it useful for studying connections between changes in emissions and changes in concentrations and damages.

Methods

The primary innovation of this paper is creating the ISRM, a dataset containing estimates of linear relationships between marginal changes in emissions at every source location and marginal changes in annual-average $PM_{2.5}$ concentrations at receptor locations. Because of computational intensity, our approach would be infeasible using a conventional air pollution model. We built the ISRM by running InMAP >150,000 times (7), each time inputting a 1-t emission change from a single grid cell. In total, our analyses required 46 d of model run time. An analogous set of runs using a CTM would take ~2,000 y with contemporary computational software based on the Weather Research and Forecasting/Chem model configuration used to inform InMAP (29) (see *SI Appendix*, section S2 for details). The results of each InMAP run describe the isolated impact of a 1-t emission change at the source upon $PM_{2.5}$ concentrations at every receptor grid cell in the model. This process is repeated for all 52,411 grid cells in InMAP and for each of three effective emission heights: ground level (emissions between 0 and 57 m), low (57–379 m), and high (>379 m). InMAP is designed with grid cell sizes that, for computational efficiency, vary based on spatial gradients in population density. The primary grid cell unit is 48 km × 48 km and is used in sparsely populated regions to achieve greater computational efficiency. For areas with progressively denser populations, the grid cells have dimensions with 24-, 12-, 4-, 2-, and 1-km sides. The ISRM, as described here [version 1.2.1, freely available for download at zenodo.org (28)], was created using InMAP version 1.2.1 (https://github.com/spatialmodel/inmap).

Here, we estimate the marginal monetary damages associated with premature mortality owing to emission of an additional t of a pollutant at a location. We adopt a linear C-R function to convert changes in $PM_{2.5}$ concentrations into adult all-cause premature mortality (8). We use the US EPA recommended VSL of $8.3 million in year-2011 US dollars to assign monetary values to changes in the risk of mortality caused by pollution (9). To calculate total damages, we multiply marginal damages by the total anthropogenic emissions in each grid cell, taken from the US EPA 2011 NEI (12). We estimate anthropogenic emissions of each of the five pollutants for each InMAP grid cell, each emission height, and each of 12 sector groupings. Additional details on the methods are in *SI Appendix*, section S1.

1. Dockery DW, et al. (1993) An association between air pollution and mortality in six U.S. cities. *N Engl J Med* 329:1753–1759.
2. Pope CA, 3rd, et al. (1995) Particulate air pollution as a predictor of mortality in a prospective study of U.S. adults. *Am J Respir Crit Care Med* 151:669–674.
3. US Environmental Protection Agency (2009) Integrated science assessment for particulate matter (US EPA Office of Research and Development, Research Triangle Park, NC), Technical Report EPA/600/R-08/139F.
4. Lave LB, Seskin EP (1970) Air pollution and human health. *Science* 169:723–733.
5. Muller NZ, Mendelsohn R (2007) Measuring the damages of air pollution in the United States. *J Environ Econ Manage* 54:1–14.
6. Bennett DH, et al. (2002) Defining intake fraction. *Environ Sci Technol* 36:207A–211A.
7. Tessum CW, Hill JD, Marshall JD (2017) InMAP: A model for air pollution interventions. *PLoS One* 12:e0176131.
8. Krewski D, et al. (2009) Extended follow-up and spatial analysis of the American Cancer Society study linking particulate air pollution and mortality (Health Effects Institute, Boston).
9. US Environmental Protection Agency (2010) Guidelines for preparing economic analyses (US EPA Office of the Administrator, Washington, DC), Technical Report EPA 240-R-10-001.
10. Muller NZ (2014) Using index numbers for deflation in environmental accounting. *Environ Dev Econ* 19:466–486.
11. Heo J, Adams PJ, Gao HO (2016) Public health costs of primary $PM_{2.5}$ and inorganic $PM_{2.5}$ precursor emissions in the United States. *Environ Sci Technol* 50:6061–6070.
12. US Environmental Protection Agency (2013) *The 2011 National Emissions Inventory* (US EPA Office of Air Quality Planning and Standards, Research Triangle Park, NC).
13. Paolella DA, et al. (2018) Effect of model spatial resolution on estimates of fine particulate matter exposure and exposure disparities in the United States. *Environ Sci Technol Lett* 5:436–441.
14. US Environmental Protection Agency (2011) AirData. Available at https://aqs.epa.gov/aqsweb/airdata/download_files.html. Accessed October 26, 2016.
15. Boylan JW, Russell AG (2006) PM and light extinction model performance metrics, goals, and criteria for three-dimensional air quality models. *Atmos Environ* 40:4946–4959.
16. Nasari MM, et al. (2016) A class of non-linear exposure-response models suitable for health impact assessment applicable to large cohort studies of ambient air pollution. *Air Qual Atmos Health* 9:961–972.
17. Marshall JD, Teoh SK, Nazaroff WW (2005) Intake fraction of nonreactive vehicle emissions in US urban areas. *Atmos Environ* 39:1363–1371.
18. Greco SL, Wilson AM, Spengler JD, Levy JI (2007) Spatial patterns of mobile source particulate matter emissions-to-exposure relationships across the United States. *Atmos Environ* 41:1011–1025.
19. Humbert S, et al. (2011) Intake fraction for particulate matter: Recommendations for life cycle impact assessment. *Environ Sci Technol* 45:4808–4816.
20. Fann N, et al. (2012) Estimating the national public health burden associated with exposure to ambient PM2.5 and ozone. *Risk Anal* 32:81–95.
21. Institute for Health Metrics and Evaluation (2015) GBD compare (IHME, University of Washington, Seattle). Available at https://vizhub.healthdata.org/gbd-compare/. Accessed May 11, 2016.
22. National Research Council (2010) *Hidden Costs of Energy: Unpriced Consequences of Energy Production and Use* (The National Academies Press, Washington, DC).
23. Fann N, Fulcher CM, Baker K (2013) The recent and future health burden of air pollution apportioned across U.S. sectors. *Environ Sci Technol* 47:3580–3589.
24. Viscusi WK, Aldy JE (2003) The value of a statistical life: A critical review of market estimates throughout the world. *J Risk Uncertain* 27:5–76.
25. Kochi I, Hubbell B, Kramer R (2006) An empirical Bayes approach to combining and comparing estimates of the value of a statistical life for environmental policy analysis. *Environ Resour Econ* 34:385–406.
26. Cropper M, Khanna S (2014) How should the World Bank estimate air pollution damages (Resources for the Future, Washington, DC), Technical Report RFF DP 14-30.
27. Centers for Disease Control and Prevention, National Center for Health Statistics. (2018). Available at https://wonder.cdc.gov/ucd-icd10.html. Accessed December 31, 2018.
28. Dataset available at zenodo.org. Available at https://doi.org/10.5281/zenodo.2589760.
29. Tessum CW, Hill JD, Marshall JD (2015) Twelve-month, 12 km resolution North American WRF-Chem v3.4 air quality simulation: Performance evaluation. *Geosci Model Dev* 8:957–973.